Chapter 11

11 T dipole and new connection cryostat for the dispersion suppressor collimators

F. Savary[1*] *and D. Schoerling*[1]

[1]CERN, Accelerator & Technology Sector, Switzerland
[*]Corresponding author

11 11 T dipole and connection cryostat for the dispersion suppressor collimators

11.1 Introduction

In Run 3 the intensity of the ion beams (usually Pb ions) for ion–ion collisions is planned to be increased by a factor of three: from 40×10^9 to 120×10^9 circulating particles. This intensity increase will amplify the losses in the cold zone at P2 and P7 and may drive the beam induced heat losses in the main dipoles in the dispersion suppressor (DS) region above the quench limit. To avoid limiting the machine performance during ion operation due to this effect, various countermeasures have been studied, and the solution chosen was to intercept these diffractive losses via warm absorbers, so-called TCLDs (Target Collimator Long Dispersion) suppressors, left and right of the LHC interaction points P2 and P7.

The concerns about diffractive losses of the Run 3 ion as well as later physics runs are reinforced by the high diffractive losses in IR7 collimators for the proton runs with beam intensity above nominal. At HL-LHC intensity, after LS3, a TCLD in the dispersion suppressor region left and right of IR7 is needed. For Run 3 intensity, with bunch populations of 1 - 1.7 10^{11} p we will be probably in a grey area, given by the uncertainties of the simulations. The paramount importance of the proton run (a limitation in DS losses would directly affect directly the luminosity reach of the ATLAS and CMS experiments), has reinforced the decision of advancing the installation of the 11 T and associated TCLD collimators to intercept the diffractive losses in the DS for both, ion and protons run. A detailed description for the reasons of the change for P2 and P7 is given in Refs. [1] and [2], respectively.

For P2, a detailed analysis of the losses has shown that the most effective place to install the TCLDs is at the centre position of the existing connection cryostats (LEBR.11L2, LECL.11R2). The positions are:

- LEBR.11L2: distance from IP2: - 432.1047 m, distance from IP1 (DCUM): 2900.2557 m.
- LECL.11R2: distance from IP2: 419.33 m, distance from IP1 (DCUM): 3751.6904 m.

This change requires the removal of the present so-called ‘empty’ cryostat LEBR.11L2 and the installation of the connection cryostat full assembly at the LEBR place. The assembly is composed of two new connection cryostats (shorter in length), with a bypass cryostat installed between them. After that, installation of a new TCLD collimator between the two connection cryostats follows. WP11 delivers the two new connection cryostats and the bypass cryostat. A detailed description of the required changes in the LHC is given in Ref. [3].

For P7, it was found that the only effective and available place to install the collimator is at the position of an existing main dipole magnet (MB). In order to make the installation of a TCLD at such a location possible and considering technological constraints, magnets with a nominal operating field of 11 T based on Nb_3Sn

technology were proposed and consequently developed. By replacing MBs (nominal field of 8.33 T), with 11 T dipoles, also called MBH, the same integrated field can be generated on a length which is around 3.5 m shorter. This gained space is sufficient to place a by-bass cryostat with a TCLD collimator assembly. For reasons of beam dynamics (reduction of the orbit excursion with respect to the ideal trajectory) and to reduce the technology risk associated with the innovative and relatively expensive Nb_3Sn superconductor, it was decided to split the MBH into two straight magnets of 5.5 m length each, with the bypass and collimator module installed in the middle. The development of the MBH magnet was initiated at FNAL in October 2010 and in the middle of 2011 at CERN. The performed R&D at FNAL and at CERN is discussed in detail in Refs. [4] and [5], respectively.

The final number and position of MBs and the scope of the project at both FNAL and CERN was realigned due a re-evaluation of heat deposition, modified beam optics, and a change in the funding profile. In August 2019, the final baseline for the installation of the MBHs was formally approved [6]. According to this baseline, the standard LHC dipole magnets MB.A9L7 (LBBRB.9L7) and MB.A9R7 (LBARA.9R7) are replaced with MBHs. The positions are (virtual interconnect plane, upstream B1):

- MB.A9L7 (LBBRB.9L7): distance from IP7: -323.629 m, distance from IP1 (DCUM): 19670.5334 m, half-cell 9.L7, called following P7 left side.
- MB.A9R7 (LBARA.9R7): distance from IP7: 307.969 m, distance from IP1 (DCUM): 20302.1314 m, half-cell 9.L7, called following P7 right side.

In detail, the changes comprise the removal of the present MBs, the installation of the 11 T dipole full assembly at the MB place. The assembly is composed of two dipoles and a bypass cryostat in the middle, providing cryogenic and electrical continuity between them. After that, the installation of a new TCLD collimator between the two magnets will follow. A detailed description of the required changes in the LHC is given in Ref. [2].

11.2 The connection cryostat full assembly

On both sides of IR2, the existing connection cryostat cryo-assembly will be replaced with a string of three independently installed and aligned cryo-assemblies: two of these will be new connection cryostats (QEP), with a bypass cryostat (QEN) installed between them. This new assembly will be called connection cryostat full assembly. There are two types of cold masses per cryo-assembly: the cold mass QEP_001 that will be installed on the left hand side of the collimator (for an observer looking from the centre of the accelerator), and the cold mass QEP_002 that will be installed on the right hand side of the collimator. These cold masses will have all the features to make their installation compatible with the location of the collimators on either side of the IR2. The QEP cold mass assembly has a length of 5309 mm between the datum plane C and L at the end covers. The QEPs need to be compatible with the LHC lattice and its main systems. They will be connected in series with the MBs and MQs. The cold mass of the QEP is made of a mechanical structure holding several pipes ensuring continuity of the cryogenic circuits. Specific busbars are installed inside the cold mass for continuity of the main and auxiliary powering circuits. The mechanical structure is based on three 25 mm thick stainless-steel plates assembled with screws to form an H type beam. This beam is reinforced by intermediate plates to ensure mechanical stability of the assembly when loaded. A cross-section through the QEP is shown in Figure 11-1.

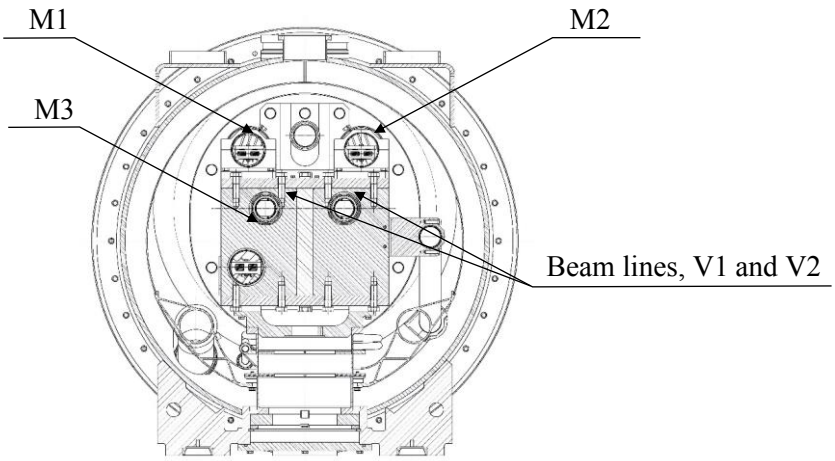

Figure 11-1: Cross-section of the QEP.

The cold mass is finished by a flat plate on the side of the assembly facing the existing MBs or MQs (see Figure 11-2) and by a dished end of a larger diameter on the side of the assembly facing the collimator (see Figure 11-3).

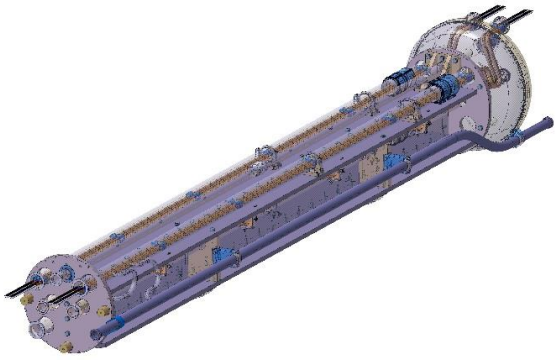

Figure 11-2: QEP Cold Mass (MBs side)

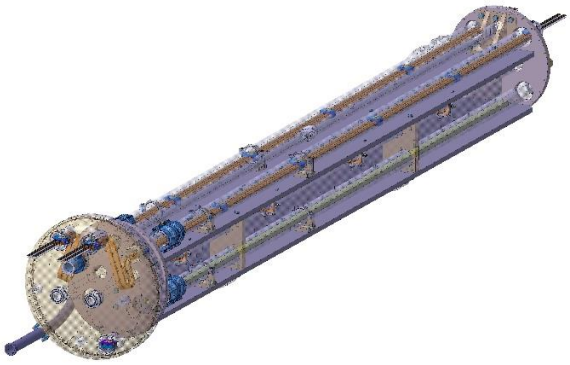

Figure 11-3: QEP Cold Mass (QEN side)

The cryogenic circuit is composed of three pipes housing the main busbars and a heat exchanger pipe connected to a "shuffling module" composed of two dished ends. On the MBs or MQs side, the pipes housing the busbars are placed in the same position as in a standard interconnection. On the collimator side, the busbars are placed further away from the beam lines to allow the routing of the busbars across the bypass cryostat. The shuffling module is made large enough to hold the lyras of the busbars and is used also to make the transition between the position of the busbar in a standard interconnection and their position in the bypass cryostat.

The QEP will be equipped with the same cold bore tube and beam screen as the present connection cryostats to facilitate integration. The cold bore is installed inside a larger pipe hydraulically connected to the main cryogenic circuit of the QEP to ensure low temperature cryo-pumping on the beam vacuum surface. This configuration guarantees the temperature of the cold bore walls to be at 1.9 K in operation.

Contrary to the connection cryostats installed presently in the LHC, which features a Pb shielding for protecting the busbars and downstream magnet from particle radiation, the QEP has no such shielding installed, as it was deemed not necessary (see Ref. [7]).

The main parameters of the QEP are listed in Table 11-1.

Table 11-1: Main parameters of the QEP.

Characteristics	Unit	Value
Cold bore tube inner diameter/thickness	mm	50/1.5
Number of apertures	-	2
Distance between apertures at room temperature/1.9 K	mm	194.52/194.00
Cold mass physical length (between datum planes C and L)	m	6.252
Cold mass weight	kg	~2000
Nominal operating current (main circuit busbars)	kA	11.85
Operating temperature	K	1.9
Heat exchanger hole inner diameter	mm	60
Heat exchanger distance from centre (same position as in the MB)	mm	180

Full reference to the integration is given in Ref. [8] and the information for installation in the HL-LHC is provided in Ref. [3].

11.3 The 11 T dipole full assembly

A main dipole cryo-magnet assembly (MB) will be replaced with a string of three independently installed and aligned cryo-magnet assemblies: two of these will each house an 11 T dipole, referred to below as the MBH, with a bypass cryostat installed between them. This new assembly will be called 11 T dipole full assembly. The bypass cryostat ensures the continuity of the cryogenic and electrical circuits and comprises cold to warm transitions on the beam lines in order to create a room temperature vacuum sector sufficiently long to install the TCLD. The TCLD is supported directly from the tunnel floor so as not to be affected by deformations of the cryostat vacuum vessels due to alignment or pressure-induced forces. A pair of MBHs will provide an integrated field of 119 T·m at the nominal operating current of the MBs, 11.85 kA. This corresponds to a nominal magnetic flux density of 11.23 T at the centre of the bore. This goal shall be obtained with a margin of ~20% on the magnet load line. A detailed description of the 11 T magnet is provided in the next Section.

Figure 11-4 shows a schematic layout of the string of cryo-assemblies composing the 11 T dipole full assembly, which will replace a main dipole cryo-magnet assembly. The cryostat for the MBH follows the same design and fabrication principles as the other arc cryostats. It complies with the static heat loads specified by the Heat Load Working Group [9]. Standard LHC cryostat performance in terms of alignment tolerances and geometrical stability are ensured. The design of the bypass cryostat is compatible with the integration of the collimator and of the RF-shielded gate valves at the extremity of the cold-to-warm transitions shown in Figure 11-5. All cryogenic lines and powering busbars have their continuity ensured across the bypass cryostat. Enlarged end covers at the extremity of the MBH cold mass interfacing with the collimator allows for all lines to run straight across the bypass cryostat as illustrated in Figure 11-6.

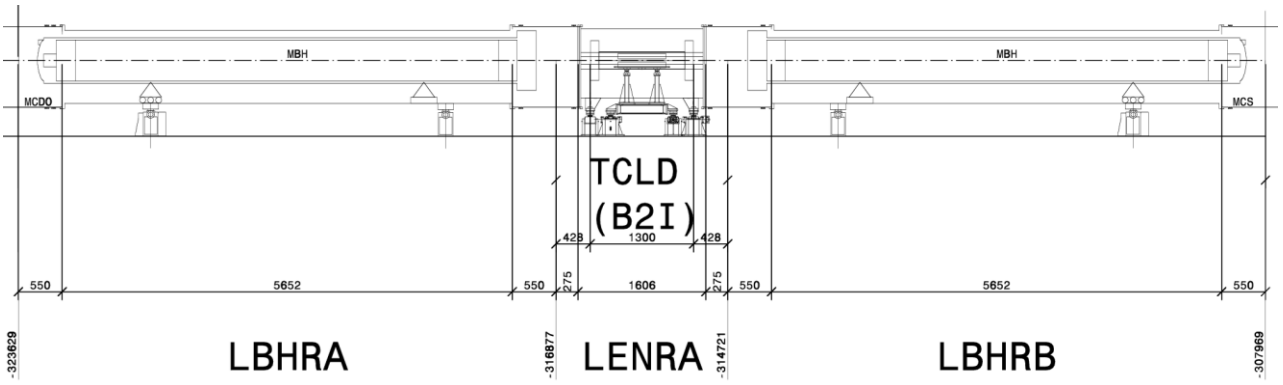

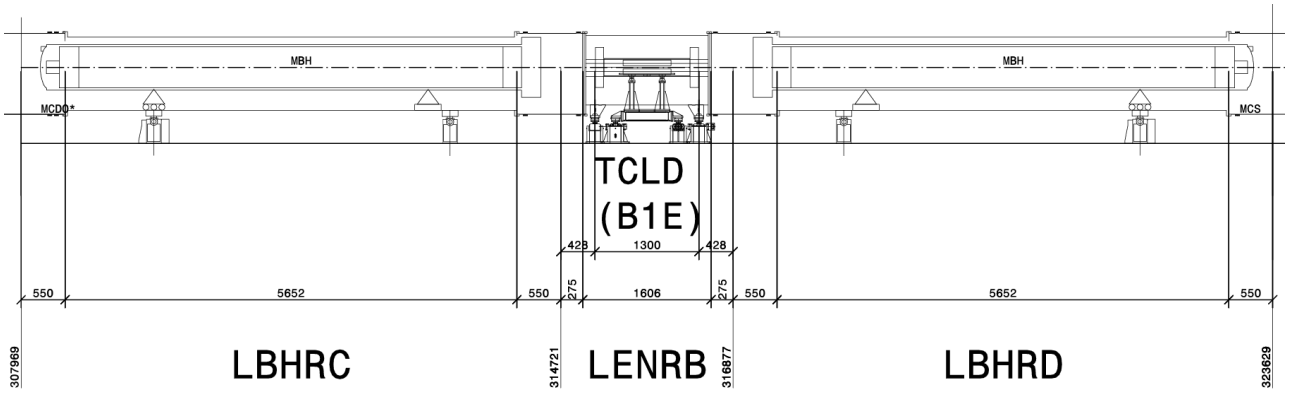

Figure 11-4: Section of the HL-LHC layout for P7 left (from LHCLSSH_0013, top) and P7 right (from LHCLSSH_0014, bottom).

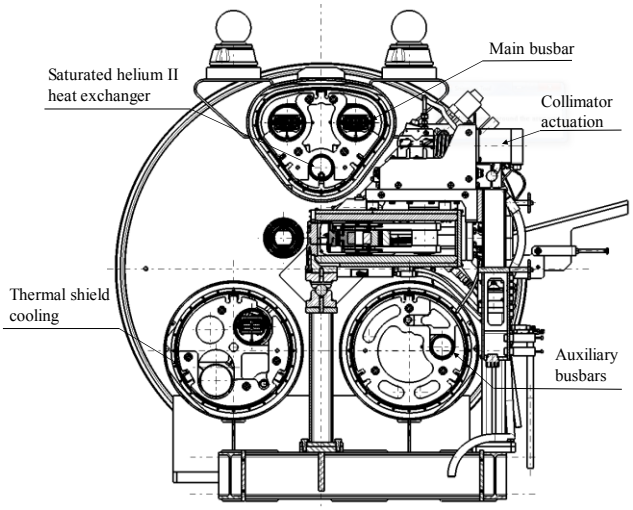

Figure 11-5: Cross-section of the bypass cryostat and collimator. The three main busbar lines have been moved away from the beam lines radially in order to create space for the collimator and the beam vacuum sector valves.

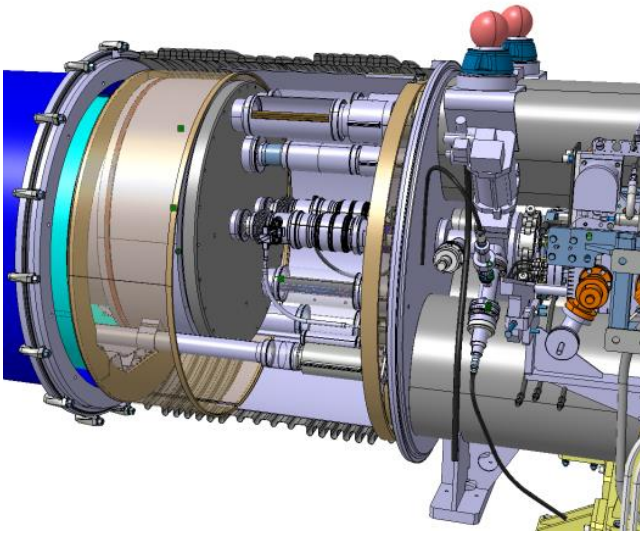

Figure 11-6: View of the enlarged cold mass end cover and the interconnection to the bypass cryostat .

The main parameters of the 11 T dipole full assembly are given in Table 11-2. The dimensions of the cryogenic pipes are equivalent to those of a standard LHC arc continuous cryostat.

Table 11-2: Main parameters of the 11 T dipole full assembly.

Characteristics	Value (mm)
Total length including interconnects	15660
Upstream cryostat length between interconnect planes	6752
Downstream cryostat length between interconnect planes	6752
Bypass cryostat length between interconnect planes	2156
Beam line cold bore diameter (inner)	50
Length of room temperature beam vacuum sector measured between cold-to-warm transition flanges	1230
Compatible active length of the collimator jaws	600

The design of the 11 T dipole full assembly is based on the following baseline.

- The length of the jaws of the collimator is 600 mm and this is valid for all the locations envisaged for installation, in particular for proton and ion cleaning (see Chapter 5).
- The interface between the cold beam lines of the MBH cryostats and the beam vacuum sector of the collimator requires sectorization by RF-shielded gate valves.
- As opposed to other collimators in the machine, residual radiation to personnel is assumed compatible with the removal and installation of the TCLD collimator without remote handling equipment. Given the integration constraints in the LHC dispersion suppressors, the design of a collimator compatible with remote handling is most likely not achievable.
- Radiation doses on the cryostat throughout the HL-LHC lifetime are compatible with the usage of LHC standard cryostat materials.
- Magnetic shielding is not required on the bypass cryostat. It is assumed that the magnetic field created by the busbar currents will not be detrimental to the accuracy of the TCLD instrumentation and controls.

11.3.1 The 11 T dipole

The design of the MBH is based on the two-in-one concept, i.e. the cold mass comprises two apertures in a common yoke and shell assembly, as shown in Figure 11-7. There are two types of cold mass per 11 T dipole full assembly, the cold mass LMBHA that will be installed on the left-hand side of the collimator (for an observer looking from the centre of the accelerator), and the cold mass LMBHB that will be installed on the right-hand side of the collimator. These cold masses will have all the features to make them compatible to the installation locations on either side of IP7.

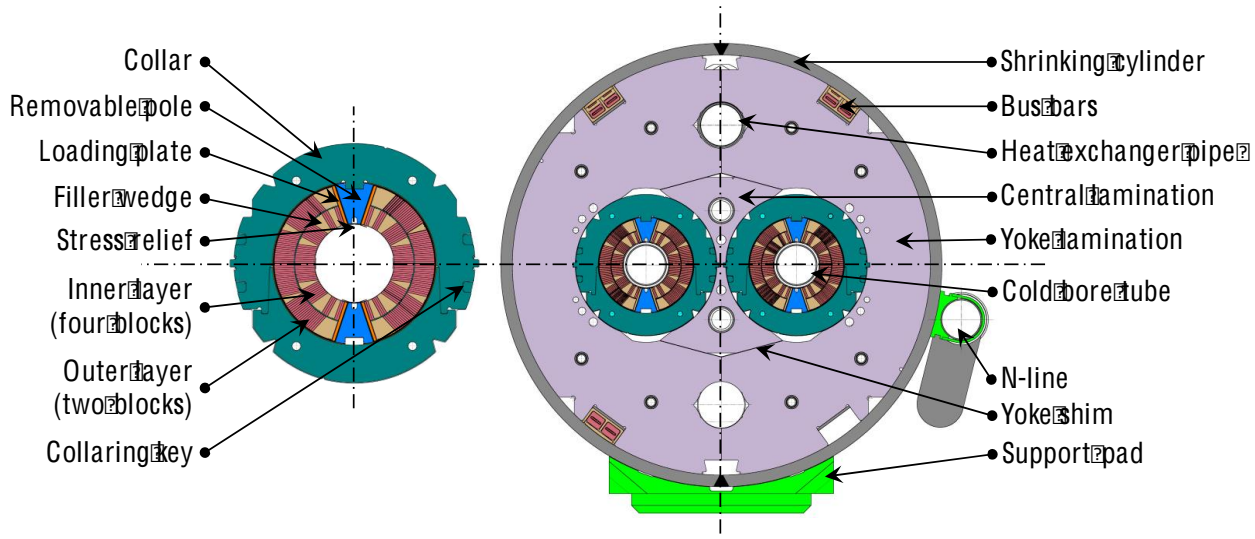

Figure 11-7: Cross-section through (left) the 11 T dipole collared coil; (right) the cold mass assembly.

The LMBH cold masses have a length of 6.252 m between the datum planes C and L that are shown on the end covers, see Figure 11-8 and Figure 11-9. The coils have a length of 5.4568 m without the outermost end spacers (called saddles), and 5.599 m with the saddles, see Figure 11-10. A pair of MBHs is needed to produce an integrated field of 119 T·m at 11.85 kA, which corresponds to the bending strength of the MB. The MBHs need to be compatible with the LHC lattice and its main systems. They will be connected in series with the MBs main dipole circuit. A detailed description of the design, technology and the performance of short models and a first full-scale prototype is given in Ref. [5]. A full-scale series magnet has been manufactured. This magnet was fully qualified for installation. After its initial training and a thermal cycle, this magnet reached nominal operating conditions without quench.

The parameters of the strands and the Rutherford cable were selected based on the required number of ampere-turns to generate the requested integrated transfer function (ITF) under the 20% operating margin, the available coil space, and the maximum number of strands possible in the cabling machine. For this last constraint, the most stringent limits were between CERN (40 strands), and FNAL (42 strands). The selected strand diameter was 0.7 mm, with a cable mid-thickness of 1.25 mm and 1.3 mm before and after reaction. As baseline strand, used for all MBH to be installed in the HL-LHC the conductor RRP 108/127 was chosen. An overview of the different conductors used for models and a discussion on the selection of this option is provided in Ref. [5]. The optimization of the cable parameters was done jointly by FNAL and CERN [10], and included the selection of the cable cross-section geometry and compaction to achieve good mechanical stability of the cable and acceptable critical current degradation (less than 10%), incorporating a stainless-steel core (25 μm thickness), and preserving a high residual resistivity ratio (RRR) of the Cu matrix (RRR larger than 100 in extracted strands).

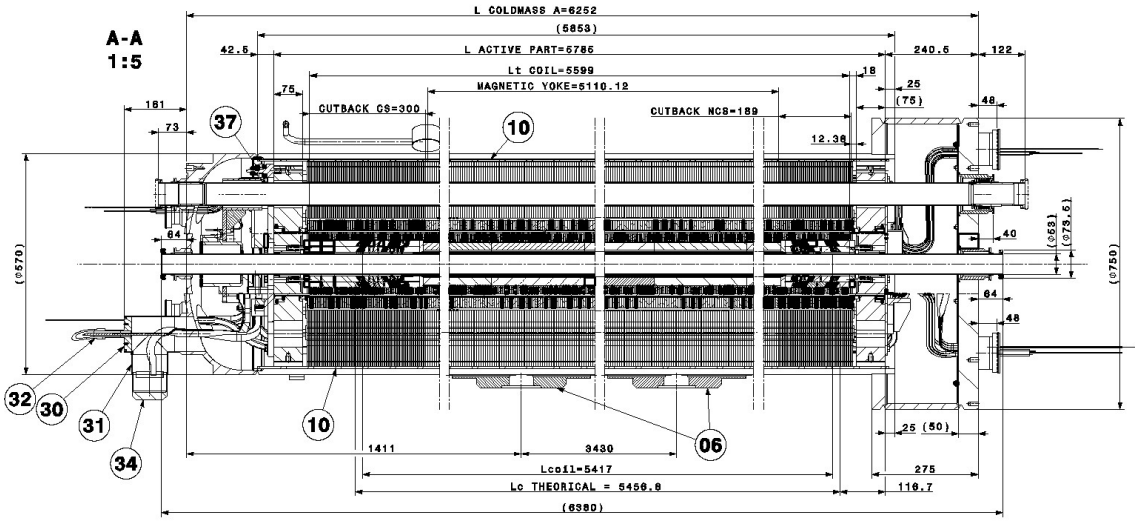

Figure 11-8: Longitudinal section of the cold mass assembly LMBHA (LHCLMBH_0001)

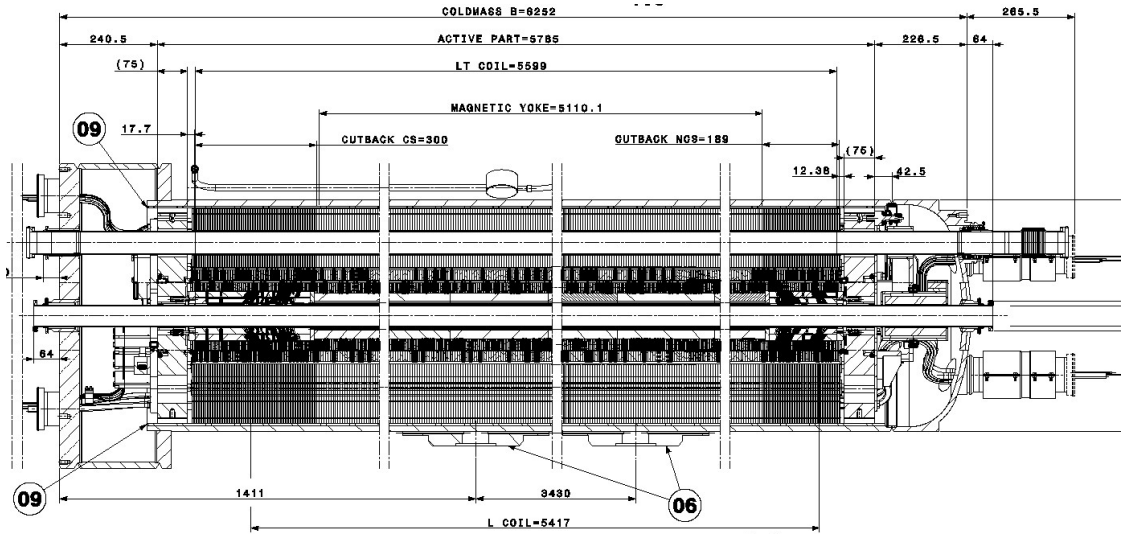

Figure 11-9: Longitudinal section of the cold mass assembly LMBHB (LHCLMBH_0002)

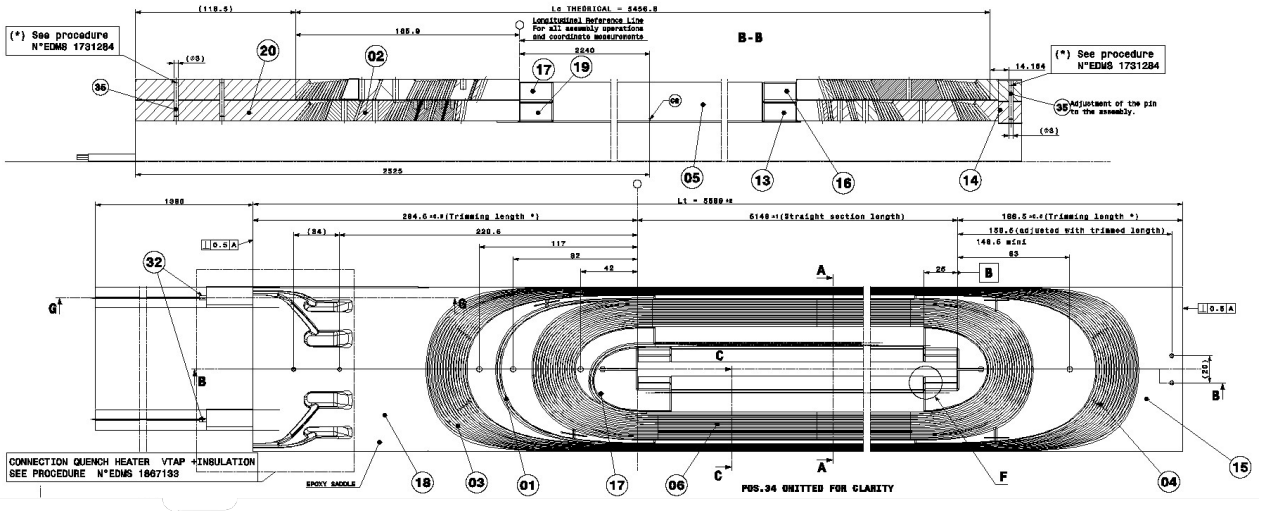

Figure 11-10: Top and side views of the coil (LHCMBH_C0005)

The first 11 T dipole series magnet was cold tested (aka S1 – MBHB-002) in Summer 2019 [11]. After the first cool down, MBHB-002 reached 11950 A (nominal current of 11850 A + 100 A margin) after 2 quenches (quench #1: 7.2 kA, #2: 11.1 kA) at 1.9 K. During the remainder of the first and second cool down, MBHB-002 always performed stable and without quench. In twothe two cold test periods cool downs combined, the magnet was ramped 370 times including 340 fast cycles. Also, at 4.5 K the nominal current + margin was reached without quench in after both cool downs. Multiple holding current tests with up to 12 hours at nominal current showed stable magnet behaviour. The results of this cold testing in combination with conform electrical high-voltage testing, have qualified this magnet for installation in the HL-LHC.

The next series magnets, S2 – MBHA-001, S3 – MBHA-002, and S4 – MBHB-003, were also tested. S2 and S4 with satisfactory results during the initial training, and S3 with unsatisfactory results, as illustrated in Figure 11-11. The magnet S3 has shown limitation in one of the coils, even if it reached 11.95 kA.

Subsequently, during the following cool downs, the magnet S2 has also shown degradation of its performance after the third cool down, CD3, with further degradation after the fourth cool down, CD4, as shown in Figure 11-12. Whereas the magnet S4 has shown degradation after the second cool down, CD2, as shown in Figure 11-13. Investigations and analysis work are on-going in order to understand the cause of the degradations observed after powering and thermal cycles.

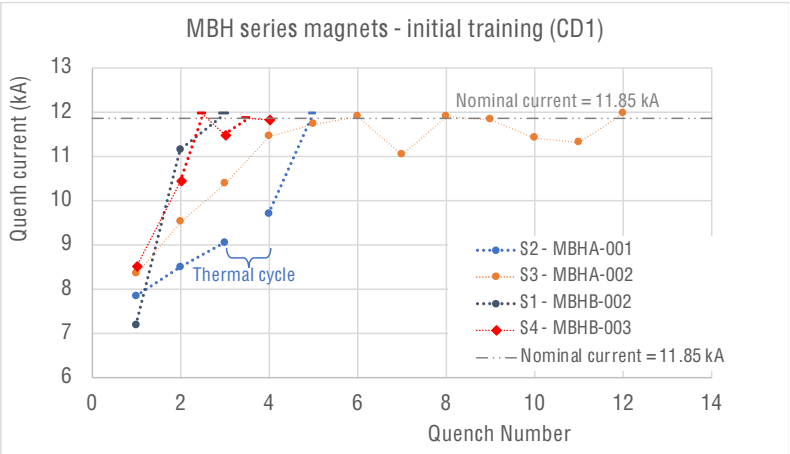

Figure 11-11: Initial training of the first 4 series magnets, i.e. first cool down or CD1. The straight markers mean no quench (S1, S2, and S4). For the magnet S2, the initial training, CD1, was interrupted in order to replace the capillary tube of the IFS because of a suspicion of electrical fault, and the cold tests were resumed after replacement of the capillary tube

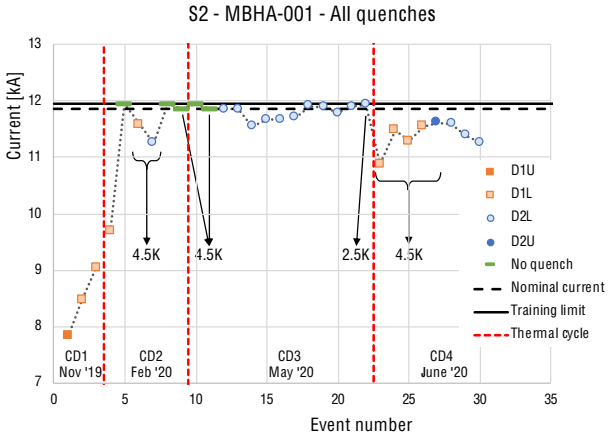

Figure 11-12: All quenches history of the magnet S2, from CD1 to CD4. Unless otherwise stipulated on the graph, the test temperature is 1.9K. The straight markers mean no quench.

D1U denotes upper coil of Aperture 1, and D1L lower coil of Aperture 1. D2U denotes upper coil of Aperture 2, and D2L lower coil of Aperture 2

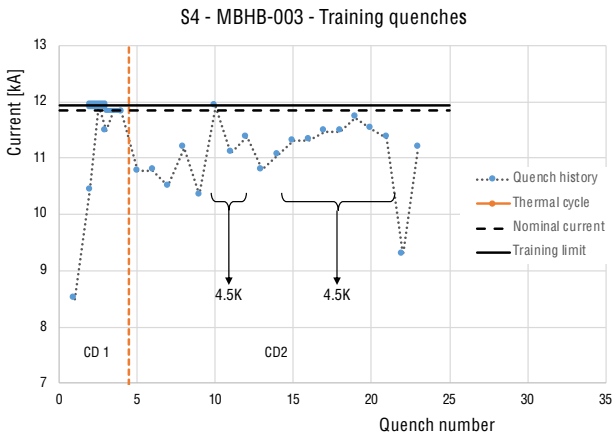

Figure 11-13: Training quenches of the magnet S4, for CD1 and CD2. Unless otherwise stipulated on the graph, the test temperature is 1.9K. The straight markers mean no quench

The main parameters of the MBH, the cryogenics, the strand and the cable are listed in Table 11-3.

Table 11-3: Main parameters of the MBH.

	Characteristics	Unit	Value
Magnet parameters	Aperture	mm	60
	Number of apertures	-	2
	Distance between apertures at room temperature/1.9 K	mm	194.52/194.00
	Cold mass outer diameter	mm	570
	Magnetic length	m	5.307
	Coil physical length, as per magnetic design	m	5.457
	Magnet physical length: active part (between the end plates)	m	5.785
	Magnet physical length: cold mass (between datum planes C and L)	m	6.252
	Cold mass weight	kg	~ 8000
	Nominal operatingoperation current	kA	11.85
	Bore field at nominal current	T	11.23
	Peak field at nominal current	T	11.77
	Operating temperature	K	1.9
	Load line margin	%	20
	Stored energy/m at I_{nom} in both apertures	MJ/m	0.896
	Differential inductance/m at I_{nom}	mH/m	11.97
	Number of layers	-	2

	Number of turns (inner/outer layer)	-	56 (22/34)
	Characteristics	**Unit**	**Value**
Cryogenics	Heat exchanger hole diameter	mm	60
	Heat exchanger distance from centre (same position as in the MB)	mm	180
	Cold bore tube inner diameter/thickness (same as in the MB)	mm	50/1.5
	Gap CBT to coil	mm	2.7
Strand	Superconductor	-	Nb_3Sn
	Strand diameter before reaction	mm	0.700 ± 0.003
	Number of strands per cable	-	40
	Cu to non-Cu ratio	-	1.15 ± 0.10
	Effective filament size D_{eff}	μm	< 41
	Cu RRR, reacted but not cabled	-	> 150
	Minimum strand critical current, I_c, without self-field correction (12 T, 4.222 K)	A	438
	Minimum strand current density, J_c, at 12 T, 4.222 K	A/mm^2	2560
Cable	Cable insulation thickness per side azimuthal, before/after reaction	mm	0.155/0.100
	Cable bare width before reaction	mm	14.7
	Cable bare mid-thickness before reaction	mm	1.25
	Cable bare width after reaction	mm	15.08
	Cable bare mid-thickness after reaction	mm	1.30
	Keystone angle RRP 108/127 before reaction	degree	0.79
	Keystone angle RRP 108/127 after reaction	degree	0.81
	Cable unit length for the two layers (no layer jump splice)	m	~650
	Cu RRR, extracted from cable after reaction	-	> 100

11.3.2 RB circuit changes

To avoid deformation changes of the beam-closed orbit of the beams, the integrated transfer function of a pair of MBHs shall be identical to that of the MB. However, this is not possible across the entire range of current during ramping up to nominal current, as shown in Figure 11-14. The design is such that a pair of MBHs provides the same integrated field of 119 T·m as a standard MB at the nominal current of 11.85 kA.

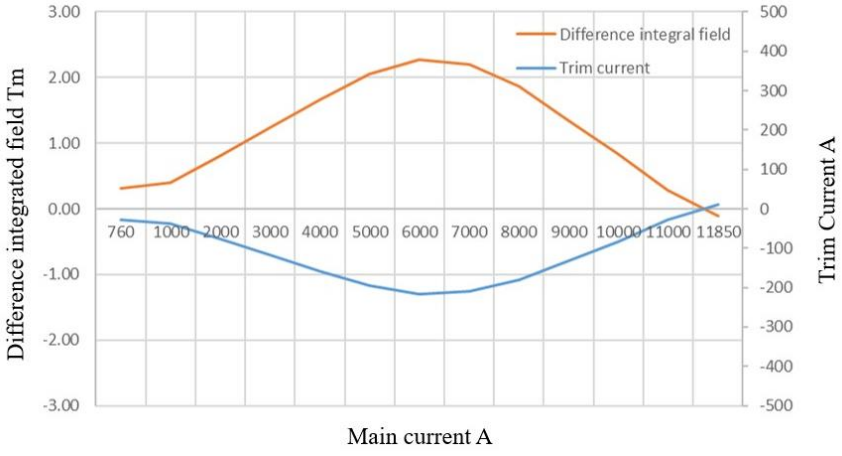

Figure 11-14: Difference in integrated field between a pair of MBHs and an MB, both delivering 119 T·m at 11.85 kA and the trim current needed to correct the difference at currents below 11.85 kA .

The MBH is stronger at lower currents (it has more turns) with a peak difference in integrated field around 6.5 kA. This can be mitigated by adding a dedicated trim power converter for ± 250 A / ± 10 V. In the absence of trim current, the resulting orbit distortion could be mitigated by means of the standard orbit correctors in the LHC lattice. Note that the MBH is assembled as a type A dipole magnet but replaces in circuit RB.A67 a MB of type B. Therefore, the circuit is adapted such that the MBH is connected into the 'A type' circuit part, leading to an asymmetric number of magnets left and right of the energy extraction. This asymmetry is considered uncritical. The MBH will be protected with quench heaters and a bypass diode operating at cold, integrated with the cold mass assembly. One bypass diode is installed for the two MBHs of an 11 T dipole full assembly, similar to the protection scheme of the MBs. The main circuit parameters are provided in Table 11-4. Further details on this circuit including all relevant references are provided in Chapter 6.

Table 11-4: RB circuit characteristics in the current LHC configuration and after the introduction of 11 T dipole full assembly for circuits RB.A67 and RB.A78.

	Circuit	**LHC Configuration**	**HL-LHC Configuration**
Maximal Required PC Voltage	RB.A67 - RB.A78	171 V	171.6 V
Total Circuit Inductance (L_{TOT})	RB.A67 - RB.A78	15.708 H	15.734 H
Circuit Time Constant (τ)	RB.A67 - RB.A78	15700s	15740s
Energy Extraction Time Constant	RB.A67 - RB.A78	112s	113s
Maximum Common Voltage of the Trim Circuit in Case of Energy Extraction	RB.A67 - RB.A78	420 V	431 V
Maximum Common Voltage of the Trim Circuit in Case of Energy Extraction + Earth Fault	RB.A67 - RB.A78	910 V	910 V

11.3.3 Instrumentation

The instrumentation foreseen in the 11 T dipole full assembly is much reduced when compared to that installed in the MBH models (1 to 2 m in length) and prototypes (full length). However, it is significantly increased when compared to the instrumentation of the standard LHC dipole of type MB that will be replaced.

The voltage taps installed along the electrical circuit are used to detect quenches in the coils and to monitor the electrical resistance of the splices between the different coils and bus bars as well as , and the electrical resistance of the joints which are part of the diode leads. The present scheme uses one V-Tap on each side of each splice in the cold mass assembly. The 14 V-Taps distributed along the dipole and spool pieces circuits inside an MBA (respectively 10 for an MBB) amount to 30 in the LMBHA, and 18 in the LMBHB. They are shown in Figure 11-15 with "EExxx" labels. This figure illustrates the 13 kA circuits, the integration of the trim circuit, and the associated V-Taps. Eighteen V-Taps are used to monitor the Nb-Ti to Nb-Ti and Nb-Ti to Nb_3Sn splices between the poles and apertures. The LMBHA cold mass is equipped with 6 additional V-Taps to monitor the joints along the diode and trim circuits, and 2 I-Taps, which can be used for specific quality control tests. Four additional wires for the MCDO and 2 for the MCS spool pieces circuits are installed respectively in LMBHA and LMBHB, as shown in Figure 11-16.

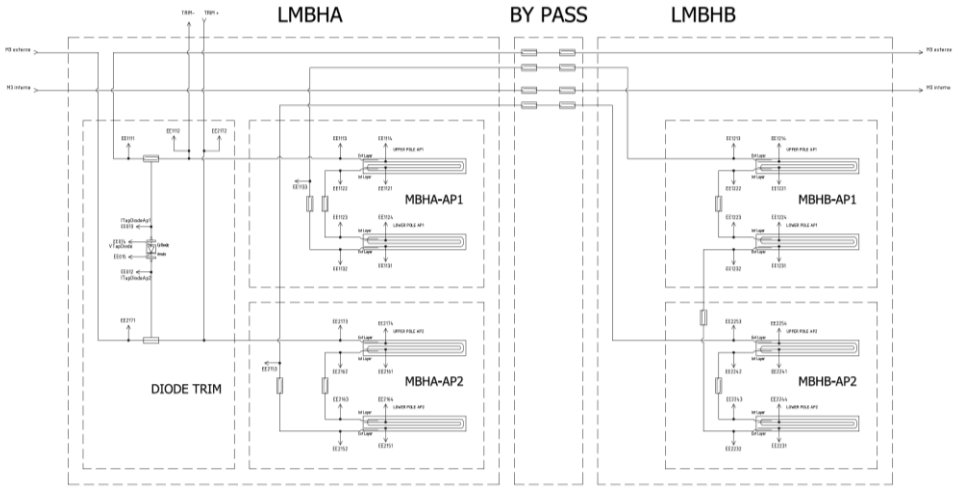

Figure 11-15: Instrumentation scheme in the main/trim circuits of the 11 T dipole full assembly substituting a standard MB (type A or type B)

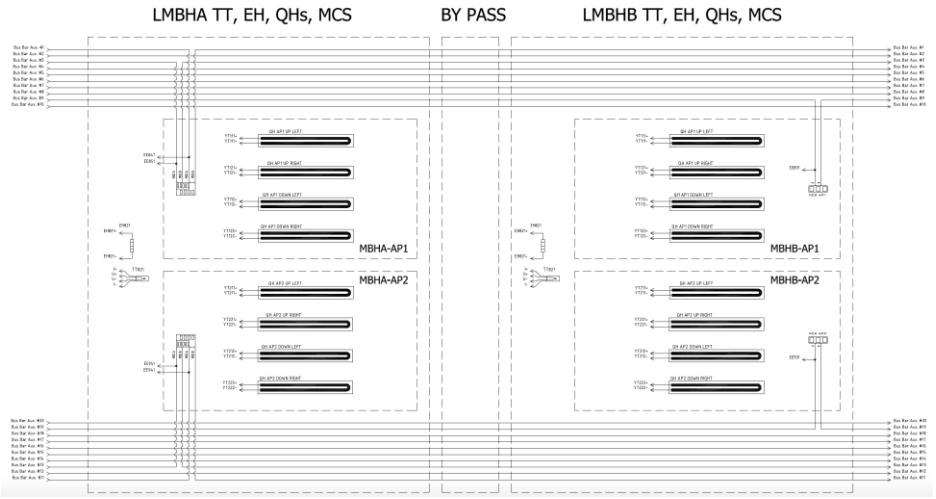

Figure 11-16: Instrumentation scheme for the temperature sensor, cryo-heater, spool pieces, and quench heaters in the 11 T dipole full assembly substituting a standard MBA.

11.3.4 Cryo-heater

A cryo-heater is installed at the bottom of each LMBHA and LMBHB cold mass on the magnet end plate at the connection side. It can be used during warm-up phases to vaporise the helium possibly remaining in the cold mass. The powering circuit of the cryo-heater comprises 2 wires.

11.3.4.1 Temperature sensor

In each LMBHA and LMBHB cold mass, a temperature sensor is attached to the lower part of the yoke, inside the magnet 2 m away from the end plate, on the connection side. It is the same as those used in the MBs (type CERNOX™). Each temperature sensor is equipped with 4 wires arranged in a cable.

11.3.4.2 Instrumentation and feed-through system

The instrumentation feed-through system (IFS) provides the path for the cabling of the electrical and cryogenic instrumentation and quench heaters via a capillary tube running from the cold mass envelope to the envelope of the cryostat.

For the sake of standardization, the design of the cover flange will be the same as that the one used in the MBs. It is equipped with 40 feedthrough pins for high-voltage and low-voltage signals. Therefore, two cover flanges (and two IFS boxes) are needed for each MBH. Moreover, because the section of the 16 quench heater wires has been increased, and there are more wires in the LMBHA, it was decided to increase the inside diameter of the capillary tube from 10 mm (which is the case in the MBs) to 12 mm.

11.3.5 Impact on beam dynamics

The bending angle of the beam is kept the same thanks to the same integrated field generated by the pair of 5.5 m-long 11 T dipoles as by a standard main dipole magnet (MB).

The field quality is worse than for the one of a standard MBs, in particular the sextupole component b_3 is larger. The latest field quality table of the 11 T dipoles can be found in Ref. [12] and the field quality of each MBH will be measured in detail at cold. Beam dynamics studies [13] have shown that the expected field quality is such to leave dynamic aperture essentially unaffected, both at injection and collision energy, given the limited number of magnets which will be installed.

The field stability is similar, as the 11 T dipoles are connected in series with the MBs, so the main current in all magnets is identical during standard operation. The trim power converters have a marginal impact. The flux jump amplitudes are too small to have a significant impact on orbit and emittance. Short lifetime dips are however to be expected, even if their amplitude should not present a risk for operation.

The same type and number of spool pieces as currently installed in the MBs will be installed in the 11 T dipoles (LBBRB.9L7: MCS, for symmetry reason a MCDO will be installed but not connected to the circuit to mimic the type B dipole; LBARA.9R7: MCS and MCDO).

Unlike the main dipoles, the 11 T magnets are straight. The exact installation position considering the sagitta is given in the layout database.

11.3.6 Operation under radiation

The MBH will, inevitably, see a shower of particles from the DS collimator. The dose estimates at the foreseen locations of the 11 T dipole full assemblies around IP7, including at the level of the cold diode, have been computed in Ref. [14]. The peak dose in the coils remains below 2 MGy and will be limited to few kGy at the level of the cold diode. These predictions rely on the assumption that 10^{17} protons are lost in IR7. These levels of radiation are acceptable for the magnet components.

11.3.7 Installation and dismantling

Full reference for the integration is given in Ref. [15] and the information for installation in the HL-LHC is provided in Ref. [2].

11.3.8 Cryogenics

11.3.8.1 Cooling

Although the cooling layout is similar to that of an MB, the heat extraction capacity in the MBH is quite different from the MBH due to construction specificities of the Nb_3Sn coils, in particular because they are impregnated and can function for coil temperatures exceeding the lambda point of helium (2.17 K). In both magnet cases, the cold source is formed by a bayonet heat exchanger protruding the upper yoke-hole. Whereas the MB has radial connections open to helium from the annular space in between the coil-inner layer and beam-pipe to this cold source, the coils of the MBH do not. Adding such radial connections in sufficient amount for a measurable improvement in effective cooling, specifically through the titanium pole of the coils, is for the moment considered not feasible. Therefore, instead of radially, the heat extraction for temperatures below the lambda point will take place via conduction over the magnet length through the helium contained in the annular

space between beam-pipe and inner-coil layer towards the magnet ends. Given a cold bore of 54.5 mm diameter (53 mm + Kapton® insulation), an inner coil diameter of 59.8 mm and a magnet length of 5.5 m, the maximum heat extraction capacity at 2.1 K is evaluated to 1.7 W/m (9.3 W total). This is approximately a factor 3 above the requirement. Therefore, radial cooling channels through the coil will not be required as long as the annular space around the beam pipe towards the magnets-ends remains unobstructed and thus free for the helium. In addition, for coil temperatures exceeding the lambda point the MBH will be able to conduct heat away through the outer coil surface across the electrical insulation layers. Assuming an electrical insulation equivalent to ~600 µm of Kapton, the heat exchange coefficient is approximately 7.7 W/K.m for the two apertures combined, i.e., 21 W per two apertures and over 5.5 m length for outer layer coil temperatures 0.5 K above the helium bath temperature.

11.3.8.2 Quench-induced pressure

In the absence of radial escape channels for the helium from the annular space around the beam-pipe an assessment of possible pressure build-up in this area has to be made. This with reference to experience with the MBs where, in case this radial escape path was blocked, dangerously high pressures develop [16][17]. We do not expect this to be an issue due to the fact that:

- The Nb_3Sn coil is fully impregnated, thus eliminating the effects due to helium in close contact with the cable;
- The helium escape path along the annular space around the beam-pipe is much wider than in the MB;
- The escape path is much shorter as the magnet is only ~5.5 m long.

11.4 Inventory of units to be installed and spare policy

Besides the units required for installation (see Section 11.1) one full spare assembly of the connection cryostat full assembly and the 11 T dipole full assembly will be produced. The components for the full assembly spare unit of the connection cryostat are available, the spare full assembly of the 11 T dipole magnets is planned to be finalized in 2021.

11.5 Quality assurance

The fabrication of the parts of the 11 T dipole full assembly and of the connection cryostat full assembly comply with the HL-LHC Quality Assurance Plan, whose implementation started at the beginning of the prototyping phase. A dedicated Quality Assurance team ensures systematic update of the relevant documentation: drawings, test reports, technical specifications, work instructions, and Manufacturing and Inspection Plans (MIP). The documentation is classified in the CERN reference databases, EDMS and CDD, where it can be easily retrieved.

Each production step is checked and documented following the MIP in order to provide adequate traceability level for each performed operation.

11.6 References

[1] R. Bruce *et al*., Installation in IR2 of dispersion suppressor collimators (TCLD), EDMS: 1973010.

[2] D. Schoerling *et al*., Installation of the 11 T Dipole Full Assembly in LHC P7 (HL-LHC WP11), EDMS: 1995306.

[3] D. Schoerling *et al*., Installation of the Connection Cryostat Full Assembly in the LHC P2 (HL-LHC WP11), EDMS: 1973010.

[4] Zlobin A.V. (2019) Nb_3Sn 11 T Dipole for the High Luminosity LHC (FNAL). In: Schoerling D., Zlobin A.V. (eds) Nb_3Sn Accelerator Magnets. Particle Acceleration and Detection. Springer, Cham, DOI: 10.1007/978-3-030-16118-7_8.

[5] B. Bordini *et al.* (2019) Nb_3Sn 11 T Dipole for the High Luminosity LHC (CERN). In: Schoerling D., Zlobin A.V. (eds) Nb_3Sn Accelerator Magnets. Particle Acceleration and Detection. Springer, Cham, DOI: 10.1007/978-3-030-16118-7_9.

[6] Summary of the 382nd LMC Meeting held on 21st August 2019, INDICO: 847537.

[7] C. Bahamonde and A. Lechner, Needs for shielding in the connection cryostats in IR2 DS, 14th TCC, 01/09/2016, INDICO: 559125.

[8] M. Gonzalez de la Aleja, WP11: Point 2 Connection Cryostat Full Assembly Integration Study, EDMS: 1904996.

[9] Heat Load Working Group, web page.

[10] A.V. Zlobin *et al*, Design and fabrication of a single-aperture 11 T Nb_3Sn dipole model for LHC upgrades. IEEE Trans Appl Supercond 22(3):4001705, 2012, DOI: 10.1109/tasc.2011.2177619.

[11] G. Willering *et al*., Cold powering tests, HCLMBHB001-CR000002, EDMS: 2211895.

[12] S. Izquierdo Bermudez, Field quality table, Intranet field quality web page.

[13] L. Fiscarelli *et al*., Field Quality of MBH 11 T Dipoles for HL-LHC and Impact on Beam Dynamic Aperture, IEEE Trans. Appl. Supercond. 28 4004005, DOI: 10.1109/TASC.2018.2792424.

[14] C. Bahamonde Castro, R2E levels for installation of 11T in cell 9, 62nd TCC meeting, INDICO: 776391.

[15] M. Gonzalez de la Aleja (WP15), WP11: 11 T Dipole full assembly integration study, EDMS: 1904620.

[16] Lebrun, P. *et al*., Investigation of quench pressure transients in the LHC superconducting magnets, 15th International Cryogenic Engineering Conference, Genoa, 1994, pp.705-708. CERN-AT-94-16-CR-MA.

[17] Wahlström, T., Investigation of quench pressure transients in the LHC superconducting magnets, 1994, CERN-AT-94-46.